

Effects of Operation Parameters on Heavy Metallic Ion Removal from Mine Waste by Natural Zeolite

Amanda L. Ciosek, Grace K. Luk

Department of Civil Engineering, Faculty of Engineering and Architectural Science, Ryerson University
350 Victoria Street, Toronto, Ontario, Canada M5B2K3
amanda.alaica@ryerson.ca; gluk@ryerson.ca

Abstract – This study investigates the effects of particle size (0.420-1.1410 mm), dosage (40, 80 g/L), influent concentration (total 10 meq/L, 400 mg/L), contact time (5-180, 270, 360 min), set-temperature (20-32°C), and heat pre-treatment (200, 400, 600 °C) of natural zeolite on the removal efficiency of heavy metallic ions (HMIs); lead (Pb^{2+}), copper (Cu^{2+}), iron (Fe^{3+}), nickel (Ni^{2+}), and zinc (Zn^{2+}). The sorption process is performed in batch mode with a 100 mL aqueous solution, acidified to a pH level of 2 with concentrated nitric (HNO_3) acid. For all experimental parameter conditions examined, the removal efficiency order follows: $Pb^{2+} > Fe^{3+} > Cu^{2+} > Zn^{2+} > Ni^{2+}$; the zeolite mineral exhibits the greatest preference towards the Pb^{2+} ion in all parameter trends. Overall, the removal efficiency is increased with decreasing particle size, as well as increasing dosage, contact time, and set-temperature. The operation is influenced by the studied parameters in the order of: influent concentration > heat pre-treatment level > dosage > particle size > contact time > set-temperature.

Keywords: Natural Zeolite, Heavy Metallic Ions, Sorption Capacity, Removal Efficiency.

© Copyright 2018 Authors - This is an Open Access article published under the Creative Commons Attribution License terms (<http://creativecommons.org/licenses/by/3.0>). Unrestricted use, distribution, and reproduction in any medium are permitted, provided the original work is properly cited.

1. Introduction

Waterways are prone to acid mine drainage (AMD) contamination caused by the discharge of mineral mining and processing effluent [1,2]. Characterized by low pH levels and the presence of heavy metallic ions (HMIs) and other toxic elements [2], AMD significantly threatens our health and environment, causing various diseases and disorders [3-5]. The process of sorption has attained the interest

of the mining industry as an industrial wastewater treatment method [6,7]. The uptake of HMIs is attributed to both adsorption (on the surface of the sorbents' micropores) and ion-exchange (through the sorbents' framework pores and channels) mechanisms [8]; referred to as sorption as a unified treatment process [9,10].

Natural zeolites have progressed among researchers' interests [6,11]. The mineral's structure is comprised of three independent components [11-13]: (1) hydro-aluminosilicate crystalline structure of SiO_4 and AlO_4 tetrahedras linked by oxygen atoms, (2) interconnected void spaces in a framework containing exchangeable cations, and (3) zeolitic water present at 10-20% of the dehydrated phase of the natural zeolites' structure. Its open, homogenous microporous negatively charged three-dimensional framework of voids and channels [11] enables the exchange with cations present when in solution [1,14]. Clinoptilolite, a globally abundant and well-documented form of zeolite [13], is used in this research. One of the most significant properties of zeolite is its high cation exchange capacity (CEC), and it is considered as a strong candidate for the removal of wastewater contaminants [15].

The industry holds great interest in the physico-chemical influential factors that dictate sorption efficiency of zeolite; which include particle size, initial concentration, pH level, and contact time. A smaller *particle size* of the sorbent material provides greater contact surface area, which improves the performance of the sorption process [5,16]; which may be attributed to diffusion as the rate-limiting step of the overall ion-exchange mechanism in the sorption process [16]. The effect of the *dosage* (solid-mass-to-solution-volume) on the uptake of HMIs is well-established. An increase in

dosage translates to an increase in the rate of uptake; although the amount sorbed per unit mass decreases, there is a higher availability of active sorption sites which sorb more HMIs from the solution [1].

The *initial concentration* of the ions influences the removal efficiency due to the availability of functional groups on the specific surface to bind with the HMIs. This is primarily the case at higher concentrations, demonstrating a higher overall uptake given that the concentration difference is the driving force to overcome mass transfer resistance to metal ion transport between the solution and the sorbent surface [5]. The *pH level* influences the dissociation of the sorbent and solution chemistry, and affects the surface charge of the sorbents and degree of ionization of different pollutants [5]. This influence of acidity is particularly the case for HMIs that are in a rather low preference by zeolite; the initial pH must be attentively selected to ensure a balance among all ionic species. The goal is to avoid precipitation; for once precipitated, the ions of interest cannot be sorbed [16].

The state of equilibrium is altered throughout the sorption process. Room temperature is preferred for analysis, although higher thermal treatment temperatures are assumed to enhance sorption capacity with increased surface activities and solute kinetic energy [1,5], by removing the 'zeolitic water' present in the framework [1]; however, the dehydration of zeolite is an endothermic process, thereby causing 'activation' of the material [12] to a certain threshold, after which may lead to the structural collapse of the mineral [1].

The *contact time* is an important factor in the relationship of pollutants and sorbents. The rapid uptake of pollutants and equilibrium is established in a specific and limited period, which demonstrates efficiency of the sorbent for treatment. The mechanism study conducted by Sprynskyy et al. [4] states that the sorption of HMIs by natural zeolite is a heterogeneous process with three distinct stages: (1) rapid uptake within the first 30 min of contact, (2) inversion due to desorption prevalence, and (3) slower increase in uptake. In the kinetic studies conducted by Motsi et al. [1], the initial stage of rapid adsorption occurs within the first 40 contact min; when all of the adsorption sites are available for cations to interact, and when the concentration difference between the influent stock and sorbent-solution interface is very high. Inglezakis et al. [14] tributes this period to ion-exchange in the micropores on the zeolite particles' surface. The predominance of desorption is most likely caused by

slower diffusion of exchangeable cations within the internal zeolite crystalline structure, and consequently these preferred ions occupy the available exchange positions on the zeolite surface. During the third stage, the gradual deceleration of sorption in the micropores is caused by poor access as well as by more intensive sorption in comparison to the particles' surface. All of these factors are significant towards establishing the performance of any sorbent material [5].

The composition of AMD is uniquely complex and contains numerous contaminants, which include heavy metals and other pollutants, and the presence of these in solution affect the overall removal potential [2,9]. The existence of HMIs in AMD is mine-specific, and the concentrations fluctuate extensively [17]. This is evident in the vast variations of expected HMI levels, such as: copper, iron, zinc, aluminum, and manganese at 0.17, 0.82, 101.2, 22.6, and 10.7 mg/L, respectively [18]; copper, iron, zinc, aluminum, manganese, arsenic, and cadmium at 12, 200, 85, 15, 15, 9 and 1 mg/L, respectively [1]; or lead, copper, iron, zinc, nickel, aluminum, manganese, arsenic and cobalt at 0.045, 5.4, 4.9, 11.5, 0.145, 32.8, 8.1, 0.004 and 0.269 mg/L, respectively [19]. In addition to HMIs, other AMD constituents, such as the variations in minerals, micro-organisms, and (weather and seasonal) temperatures, all influence the quality and quantity of AMD [19]. A majority of previous research on sorption capacity of zeolite has investigated synthetic simple solute solutions spiked in single-component systems [20], and have demonstrated greater removal performance compared to investigating actual AMD [1,20]. However, there is still limited knowledge of the sorption capacity by zeolite for heavy metals and the associated mechanisms when in various multi-component systems [14,21]. The synthetic simple heavy metal solution permits the analysis of the effects of the selected operation parameters in a controlled environment for improved quantification, and identification of the important trends in this study.

The authors have designed a four-phase research project, which investigates: (1) the effects of preliminary parameters and operative conditions (particle size, sorbent-to-sorbate dosage, influent concentration, contact time, set-temperature, and heat pre-treatment), (2) HMIs component system combinations and selectivity order with a focus on its effects on the removal of lead (Pb^{2+}) [22], (3) kinetic modelling trends [23], and (4) the design of a packed, fixed-bed, dual-column sorption treatment system [24].

The study presented in this paper refers to the first phase. In feasible treatments of industrial waste, it is essential to classify the degree of influence of each operational parameter on the overall system performance [17]. Therefore, the objective of this present study is to assess the sorption capacity of natural zeolite for the removal of five fundamental HMIs, specifically lead (Pb²⁺), copper (Cu²⁺), iron (Fe³⁺), nickel (Ni²⁺), and zinc (Zn²⁺) [18,25], combined in various component systems. The operative conditions of zeolite particle size and dosage, HMI influent concentration, contact time, set-temperature and heat pre-treatment level are all investigated. This is of great importance, in order to harness the full potential of zeolite in tertiary treatment processes.

2. Methodology

2.1. Materials and Equipment

2.1.1. Heavy Metallic Ion Influent Concentration

The removal efficiency order indicates the variation of the selectivity for each HMI [16]. Overall, this selectivity or preference of zeolite for one cation compared to another [26] is stronger for the counter-ion of higher valence, increasing with dilution of solution and strongest with ion-exchange of high internal molality [16]. Therefore, comparative analysis of various HMIs should be conducted at the same normality and temperature [16]; as executed in this study. The synthetic ion solutions are prepared from analytical grade nitrate salts of Pb(NO₃)₂ (CAS No. 10099-74-8), Cu(NO₃)₂·3H₂O (CAS No. 10031-43-3), Fe(NO₃)₃·9H₂O (CAS No. 7782-61-8), Ni(NO₃)₂·6H₂O (CAS No. 13478-00-7), and Zn(NO₃)₂·6H₂O (CAS No. 10196-18-6), respectively; dissolved in deionized distilled water. The metals are combined to maintain a total normality of 0.01N (10 meq/L) [14,16] in the following systems:

- single-component system–10 meq/L per metal (lead [Pb], copper [Cu], iron [Fe], nickel [Ni], zinc [Zn]);;
- dual-component system–5.0 meq/L per metal (lead-copper [Pb-Cu], lead-iron [Pb-Fe]);;
- triple-component system–3.3 meq/L per metal [T] (lead, copper and iron), and;
- multi-component system–2.0 meq/L per metal [M] (all five metals).

The corresponding HMI concentrations are approximately 1036 mg/L for Pb²⁺, 318 mg/L for Cu²⁺, 186 mg/L for Fe³⁺, 293 mg/L for Ni²⁺, and 327 mg/L for

Zn²⁺. In addition to maintaining a total 10 meq/L concentration, the study is also conducted at 400 mg/L initial concentration for each HMI, based on the median range of conversion from meq/L to mg/L concentrations for a majority of the HMI investigated.

The Canada-Wide Survey of Acid Mine Drainage [17] reports a seasonal average of a majority of the mines surveyed to have documented pH values ranging from 2 to 5. Consequently, the influent stock is acidified with concentrated nitric acid (HNO₃) (CAS No. 7697-37-2) to a pH level of less than 2 [27]. This study is conducted in the conservative manner, with a majority of the pH values documented to be below this reported average and within comparability. It is important to note that the mechanism of HMI uptake by natural zeolites is influenced by the pH level; shifting from ion exchange/adsorption in the acidic region to adsorption/complexation and possible precipitation in the basic region [28]. The neutralization increases the pH level to reach a threshold of solubility of the metal hydroxides; the removal may be partially attributed to precipitation (or sorption/co-precipitation) rather than just sorption [29]. With the use of highly soluble nitrate salts and by maintaining very low pH levels in the batch-mode configuration of all the experiments, the formation of inorganic ligands (such as OH⁻) is prevented and the precipitation of the HMIs is avoided [6,16]; under the testing conditions of this study.

Based on the dosage of zeolite mass to a selected 100 mL volume of aqueous solution, the HMI uptake is calculated by the following relationship [16]:

$$q_t = \frac{V \times (C_0 - C_t)}{M} \quad (1)$$

where q_t is the HMI adsorbed at time t (in meq/g or mg/g), C_0 and C_t are the initial and final HMI concentrations in solution (in meq/L or mg/L) after time t , V is the solution volume (in L), and M is the zeolite mass (in g).

2.1.2. Natural Zeolite Mineral

This study employs a natural zeolite mineral sample composed primarily of 85-95% clinoptilolite (CAS No. 12173-10-3) and is sourced by a deposit located in Preston, Idaho [30]. This sample holds a cation exchange capacity of 180-220 meq/100 g, a pH level ranging from 7-8.64. It has a maximum water retention and an overall specific surface area of 55 wt% and 24.9 m²/g, respectively. The zeolite mineral sample

is applied in its natural state, without any chemical modifications, to minimize associated costs and environmental impacts of the process investigated in this study. The particle size of the raw mineral sample ranges from 1.41 mm (pass No. 14) to 0.420 mm (retain No. 40). This sample is divided into sizes A ($d_{p,A}$) (1.190-1.410mm), B ($d_{p,B}$) (0.707-0.841 mm), and C ($d_{p,C}$) (0.420-0.595 mm) with standard mesh sieves and a mechanical shaker (Model No. Humboldt H4330; CAT No. G118-H-4330). Size D ($d_{p,D}$) (0.841-1.19 mm) has also been selected, ranging between A (pass No. 16) and B (retain No. 20). This additional size range holds the greatest percent yield within the +14-40 source and also, being a broader, coarser size range, is of interest to this study. Overall, these four divisions are selected to provide a distinct variance, based on the approximate distribution of the +14-40 source, as displayed in **Table 1**. The particles are put through a cleaning cycle, which involves thoroughly rinsing in deionized distilled water to remove residual debris and dust, and drying at $80 \pm 3^\circ\text{C}$ for 24 hr (Isotemp® Oven Model 630G; Serial No. 30300047; CAT No. 13-246-630G; 115 V; 6.5 A; 60 Hz; Fisher Scientific, USA) to remove residual moisture [31].

Table 1. Preliminary Distribution of Zeolite Supply.

	Test Sample Size (g)	1006.60	
	Sieve Gradations	Sample Distribution	
		(g)	(%)
	#14 Retain	76.5	7.6
A	#14 Pass #16 Retain	199.9	19.9
D	#16 Pass #18 Retain	181.1	18.0
	#18 Pass #20 Retain	150.9	15.0
B	#20 Pass #25 Retain	119.1	11.8
	#25 Pass #30 Retain	94.0	9.3
C	#30 Pass #35 Retain	68.1	6.8
	#35 Pass #40 Retain	48.3	4.8
	#40 Pass (PAN)	57.9	5.8
	SUM	995.8	98.9
	LOST	10.8	1.1

2. 1. 3. Analytical Equipment

Quantitative observations are conducted by analyzing the HMI concentrations in their aqueous phase with Inductively Coupled Plasma – Atomic Emission Spectroscopy (ICP-AES) technology (Optima 7300 DV, Part No. N0770796, Serial No. 077C8071802, Firmware Version 1.0.1.0079, Perkin Elmer Inc.), with corresponding WinLab32 Software (Version 4.0.0.0305). This spectrometry technique is considered to have true multi-element performance with

exceptional sample throughput, and with a very wide range of analytical signal intensity [32]. The primary wavelengths of each HMI element analyte targeted are 327.393 (Cu), 238.204 (Fe), 231.604 (Ni), 220.353 (Pb), and 206.200 (Zn), respectively; selected on the basis that these wavelengths have the strongest emission and provide the best quantifiable detection limits. With the plasma setting in radial view (to concentrations of greater than 1 mg/L), auto sampling of 45 seconds normal time at a rate of 1.5 mL/min, and a processing setting of 3 to 5 points per peak with 2 point spectral corrections are applied.

The calibration curve is generated through ‘linear calculated intercept’ by applying a stock blank and a multi-element Quality Control Standard 4 with 1, 10, 50, 90, and 100 mg/L concentrations (as per Standard Methods Part 3000) [27]. Based on the corresponding influent concentrations in mg/L, the samples are diluted with deionized distilled water, by zero to four pre-determined 50% steps, in order to be within this calibration range. The sorbed amount of HMI is calculated based on the initial concentration and its 0.45 μm filtered supernatant concentration.

Triplicate readings and their mean concentrations in calibration units are generated in mg/L by the ICP-AES software. Three major check parameters are selected to evaluate the calibration quality during each ICP-AES analytical session. The triplicate concentration of the median 50-mg/L standard detects an average of 51.37 mg/L, which is within 5% of the known value. The percent relative standard deviation (%RSD) of this selected standard reports an average of 0.4944% (well within the $\leq 3\%$ limit) and the correlation coefficient of each HMI analyte primary wavelength generates an average of 0.9997, which is very close to unity. These check parameters indicate that the calibration is of a reasonable level of accuracy and reliability [33], such that there is acceptable error associated with the experimental data.

2. 2. Experimental Design

All analyses are conducted in batch mode, combining the HMI solutions of various component systems to 100 mL (total 10 meq/L initial concentration) with 4 g of the zeolite sorbent mineral. The mixture is agitated on a bench-top orbital shaker with triple-eccentric drive (MaxQ™ 4450, CAT No. 11-675-202, ThermoFisher Scientific) at a controlled condition of 400 r/min set at 22°C , for a period ranging from 5 to 180 min. In all experiments, after reaction,

HMI sorbate and zeolite sorbent are separated through a 0.45 μm syringe filter. The hydrothermal pre-treatment is conducted by placing the cleaned zeolite into a pre-heated muffle furnace (NEY M-525 SII; Serial No. AKN 9403-108; 120 V; 50/60 Hz; 12.5 A; 1500 W; Barkmeyer Division, USA) at the three selected temperatures of 200°C, 400°C, and 600°C [1], for 1-hr. Table 2 summarizes the parameters investigated to determine their influence of the overall removal of the selected HMIs.

Table 2. Operation Parameters and Conditions.

Parameter	Conditions
Particle Size	Single-Component Systems: [Pb], [Cu], [Fe], [Ni], [Zn] A 1.140-1.190mm (pass No. 14, retain No. 16) B 0.707-0.841mm (pass No. 20, retain No. 25) C 0.420-0.595mm (pass No. 30, retain No. 40)
Dosage	Single-Component Systems: [Pb], [Cu], [Fe], [Ni], [Zn] Particle Size: D 0.841-1.19 mm Dosage: 4 g/100 mL, 8 g/100 mL
Influent Concentration	Systems: [Pb], [T], [M] Particle Size: D Concentrations: total 10 meq/L, 400 mg/L
Contact Time	Systems: [Pb], [Pb-Cu], [Pb-Fe], [T], [M] Particle Size D : 0.841-1.19 mm Contact Time: 180, 270, 360 min
Set-Temperature	Systems: [T], [M] Particle Size: D Contact Time: 180 min Set Temperature: 20°C, 24°C, 28°C, 32°C
Heat Pre-Treatment	Systems: [Pb], [T], [M] Particle Size: D Heat Pre-Treatment: 200°C, 400°C, 600°C

3. Results and Discussion

3.1. Particle Size and Dosage

The particle size and dosage parameters are significant to this study, as well as to the industry that adopt sorption as a treatment method. Figure 1 displays the uptake of each HMI at 180 min of contact with zeolite. As expected, with a reduction in the particle size (d_p) from A to C, the uptake and percent removal increases. This trend is most prevalent for the HMI Pb^{2+} , with a 45.63% decrease in concentration or a 15.18% increase in uptake from $d_{p,A}$ (0.1872 meq/g) to $d_{p,B}$ (0.2157 meq/g). However, this trend is not as prevalent from $d_{p,B}$ to $d_{p,C}$, with only a 3.98% in improved HMI uptake. This may be due to the greater particle size gradation range between $d_{p,A}$ and $d_{p,B}$ specifically, as well as a 40.47% decrease in nominal geometric mean diameter of 1.30 mm ($d_{p,A}$) to 0.77 mm ($d_{p,B}$). Based on the sieve distribution presented in Table 1, an average

of 10% per mesh range was detected for particle sizes B and C. In order to eliminate skater/variability, and to maintain a controlled environment, the particle size selected to observe the other experimental parameters is between A and B, denoted hereon in as size D ($d_{p,D}$). Based on these initial observations in the removal trends by particle size, the $d_{p,D}$ is considered a more feasible and conservative range moving forward; with a nominal geometric mean diameter of 1.00 mm [34].

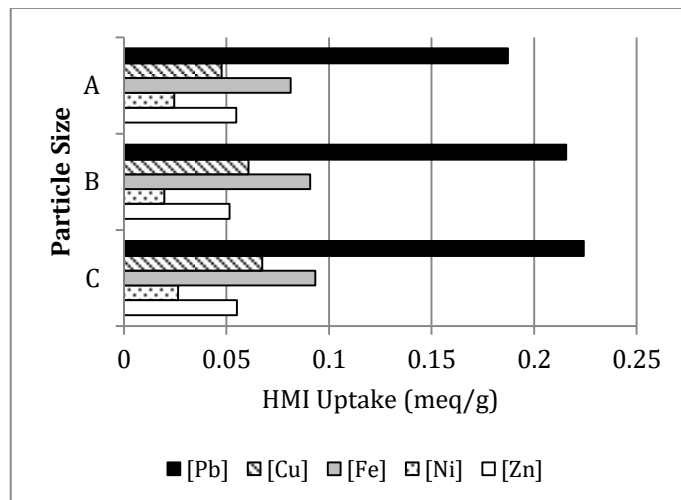


Figure 1. HMI Uptake based on Particle Size Parameter.

Figure 2 displays the overall percent removal of each HMI (in single-component solutions) at 180 min of contact with natural zeolite by increasing the zeolite sorbent dosage from 4 g to 8 g, for every 100 mL of HMI sorbate volume. As illustrated, when the dosage increases (doubled), the percent removal increases substantially; which is attributed to higher site uptake availability [35]. At a contact time of 180 min, the HMI effluent concentration is reduced for Cu^{2+} at 19.91%, Fe^{3+} at 35.93%, and significantly for Pb^{2+} at 82.37%. Additionally the overall removal efficiency of the selected $d_{p,D}$ falls within the range achieved of $d_{p,A}$ and $d_{p,B}$; demonstrating experimental continuity.

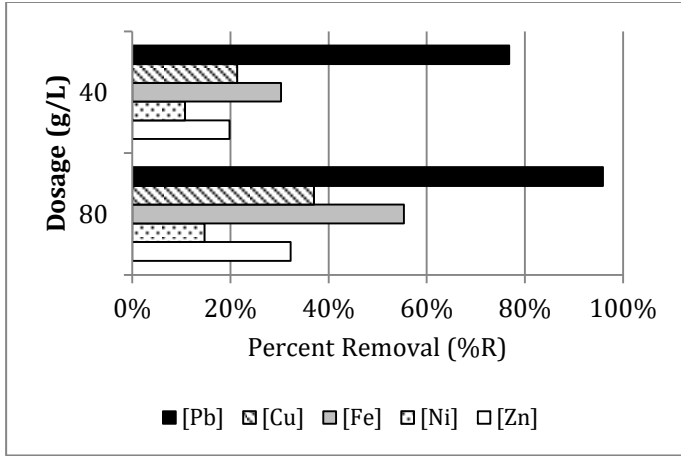


Figure 2. HMI Percent Removal based on Dosage Parameter.

Kinetic modelling is a powerful tool to assess the performance of sorbent materials and to comprehend the fundamental mechanisms involved in the sorption process. The sorption rate depends on the amount of ions on the sorbent surface at time t and what is sorbed when an equilibrium state is reached. The models are classified as either reaction-type or diffusion-type (film, intra-particle) [35]; both models have been thoroughly investigated and have demonstrated strong correlation [35-38].

The reaction-type known as the pseudo-second-order (PSO) kinetic model has well-demonstrated this rate process of various contaminants, including metal ions and organic substances in an aqueous state [36,39]. This model implies that the rate-limiting step is by chemical adsorption (chemisorption). It is represented in Eq. (2) and by applying the boundary conditions of $t = 0 \rightarrow q_t = 0$ and $t = t \rightarrow q_t = q_t$, its linearized form is presented in Eq. (3) [4,7,36,38]:

$$\frac{dq_t}{dt} = k_2(q_e - q_t)^2 \quad (2)$$

$$\frac{t}{q_t} = \frac{t}{q_e} + \frac{1}{k_2 q_e^2} \quad (3)$$

where $h = k_2 q_e^2$ is the initial sorption rate (in meq/g·min) as t approaches zero [38], and k_2 is the PSO rate constant (in g/meq·min). These constants are determined by a plot of the linearized form of t/q_t versus t [36,38]. The PSO rate constants and correlation coefficients are summarized in Table 3 and Table 4 for the particle size and dosage parameters, respectively. Based on the linearized form of Eq. (3), the slope (m) and y-intercept (b) values are interpreted to determine

the theoretical sorption at equilibrium (q_e in meq/g). The experimental sorption at 180 min (q_{180} in meq/g) of contact is also presented.

As demonstrated by the coefficients (CC), a strong correlation is established for all HMIs for both parameters. For all HMIs on average, the particle size q_{180} reaches the theoretical q_e uptake of 92.27% for $d_{p,A}$, 86.93% for $d_{p,B}$, and 93.45% for $d_{p,C}$; the dosage q_{180} reaches the theoretical q_e uptake on average of 84.27% for dosage 40 g/L and 80.72% for dosage 80 g/L. The particle size uptake rate trends in Table 3 are systematically consistent; with the $q_{e,[Pb]}$ within 5% of the theoretical maximum 0.25 meq/g threshold for total HMIs.

Table 3. PSO – Particle Size Data.

Size A					
System	q_{180}	CC	m	b	q_e
[Pb]	0.1872	0.9840	4.374	216.46	0.2286
[Cu]	0.0476	0.8193	12.780	1445.40	0.0782
[Fe]	0.0813	0.9741	11.002	372.35	0.0909
[Ni]	0.0245	0.9141	31.057	969.75	0.0322
[Zn]	0.0548	0.7413	9.569	1420.10	0.1045
Size B					
System	q_{180}	CC	m	b	q_e
[Pb]	0.2157	0.9970	3.856	147.15	0.2594
[Cu]	0.0607	0.9866	13.611	626.99	0.0735
[Fe]	0.0908	0.9934	10.190	202.53	0.0981
[Ni]	0.0196	0.9872	47.121	298.41	0.0212
[Zn]	0.0514	0.9623	16.317	795.49	0.0613
Size C					
System	q_{180}	CC	m	b	q_e
[Pb]	0.2242	0.9964	3.783	110.79	0.2644
[Cu]	0.0674	0.9700	13.942	373.99	0.0717
[Fe]	0.0933	0.9976	10.067	155.73	0.0993
[Ni]	0.0263	0.9942	37.924	274.89	0.0264
[Zn]	0.0550	0.9646	17.211	430.21	0.0581

Table 4. PSO – Dosage Data.

Dosage 40					
System	q_{180}	CC	m	b	q_e
[Pb]	0.1919	0.9926	4.098	217.01	0.2440
[Cu]	0.0533	0.9291	15.750	836.09	0.0635
[Fe]	0.0757	0.9708	11.872	419.08	0.0842
[Ni]	0.0268	0.9806	34.919	739.14	0.0286
[Zn]	0.0494	0.9147	15.237	1106.10	0.0656
Dosage 80					
System	q_{180}	CC	m	b	q_e
[Pb]	0.1198	0.9986	7.343	174.00	0.1362
[Cu]	0.0463	0.9821	17.211	926.12	0.0581
[Fe]	0.0691	0.9899	12.893	344.90	0.0776
[Ni]	0.0184	0.9967	50.300	655.14	0.0199
[Zn]	0.0403	0.6369	13.507	1771.00	0.0740

The dosage level is not directly proportional to the sorption removal efficiency. The removal efficiency of Pb²⁺ improves from 76.82% to 95.91%; however, the q₁₈₀ uptake has decreased from 0.1919 to 0.1198 meq/g, and the theoretically anticipated q_e uptake at equilibrium decreases from 0.2440 to 0.1362 meq/g, comparing dosage 40 g/L to 80 g/L, respectively. This may be attributed to the very rapid uptake of the first stage of sorption. The two HMIs preferred by zeolite in this study exhibit a faster initial sorption rate (h); for Pb²⁺ the rate increases from 0.0046 to 0.0057 meq/g·min, and for Fe³⁺ this rate increases from 0.0024 to 0.0029 meq/g·min; comparing dosage 40 g/L to 80 g/L, respectively. This finding in correlation with the lower overall expected uptake at equilibrium demonstrates that the Dosage 80 (8 g/100 mL) has reached its threshold of available active sorption sites. A higher removal at a faster rate comes at a cost of consuming more zeolite material; with the Dosage 40 (4 g/100 mL) considered more economically feasible.

In accordance with the fundamental principles of sorption (adsorption and ion-exchange), when intra-particle diffusion (IPD) as considered as the rate-limiting step, the sorption rate is proportional to \bar{D}/d_p^2 ; where \bar{D} is the diffusion coefficient of a specific HMI. Since the d_p should not affect either the equilibrium state or the \bar{D} , higher sorption rates should be observed for smaller particle sizes. However, smaller particle sizes may exhibit lower rates, due to lower effective \bar{D} values, caused by structural problems or pore clogging [21]. It is important to note that the natural (as-received) zeolite mineral sample is put through a systematic cleaning cycle, thoroughly washing before use. Therefore, pore clogging is not expected to affect the diffusion coefficients which are considered to be constant regardless of particle size. Then, with intra-particle diffusion considered as the controlling step, the exchange rate should be increased by decreasing particle size [21]; as demonstrated.

Based on the trends observed, the ideal levels of these two operation parameters (particle size d_{p,D} and 4g/L dosage) are selected moving forward in this study.

3. 2. Influent Concentration

In addition to maintaining a total 10 meq/L initial concentration, this component of the study is also conducted at 400 mg/L for each HMI, based on the median range of conversion from meq/L to mg/L concentrations for a majority of the HMI investigated

throughout this research endeavour; for single-lead [Pb], triple- [T], and multi- [M] component system combinations (Table 5).

The difference in the removal of each HMI investigated when the influent concentration is set to meq/L versus mg/L is evident. The trends detected are consistent with the literature; the amount in mg of Pb²⁺ ions available for uptake by zeolite decreases, theoretically from 1036 mg/L to 400 mg/L and the amount of the other four ions (in mg) has increased with this conversion of influent concentration. Oter and Akcay [35] demonstrated consistent findings, as the initial concentration increases, the amount of sorbed HMI increases, while the percent of sorbed HMI decreases for all ions.

Table 5. The HMI Removal Variation by Influent Concentration.

System	HMI	Total 10 meq/L			400 mg/L per HMI	
		q ₁₈₀		%R	q ₁₈₀ mg/g	%R
		mg/g	meq/g			
[Pb]	Pb ²⁺	23.31	0.192	77	9.36	95
[T]	Pb ²⁺	9.01	0.075	90	7.35	80
	Cu ²⁺	0.64	0.016	19	1.04	11
	Fe ³⁺	0.85	0.041	50	1.73	18
	TOTAL	-	0.132	-	-	-
[M]	Pb ²⁺	5.52	0.047	94	7.62	80
	Cu ²⁺	0.41	0.011	22	0.75	8.4
	Fe ³⁺	0.58	0.028	56	1.51	16
	Ni ²⁺	0.15	0.005	9.1	0.18	1.8
	Zn ²⁺	0.30	0.008	16	0.41	4.6
	TOTAL	-	0.099	-	-	-

Inglezakis et al. [16] demonstrates that dilution leads to an increase in the volume of treated solution to breakthrough (5-10% of the influent concentration) in continuous column configuration; the magnitude of which depends on the specific metal exchanged. This finding can be attributed to the increase of selectivity in the ion-exchange mechanism of sorption by dilution. The valences of the exchanging cations have a strong effect on ion-exchange at equilibrium, and consequently on the removal efficiency. This attribute is referred to as the “concentration-valency effect”. It is theoretically recognized that when the exchanging ions are not of equal valence, the equilibrium is a function of the total concentration; at higher concentrations, this process prefers the uptake of the lower charged cations and subsequently excludes higher charged cations from the sorbent [16]. The cations present in the sorbent have valences that differ from those in solution.

Consequently, as the dilution increases, the selectivity of the sorbent for the ion with a higher valence also increases. Accordingly, comparative analysis of various metal ions should be conducted at the same normality and temperature, in order to minimize the changes observed in isotherm configuration with dilution [16].

3.3. Contact Time and Set-Temperature

With [Pb], [T], and [M] component system combinations at total 10 meq/L influent concentration: (1) the contact time is extrapolated from 3 hrs to 4.5 and 6 hrs (Table 6), and (2) the set-temperature is evaluated to an adjusted range of 20 to 32°C at 180 contact min (Table 7).

Table 6. The HMI Removal Variation by Contact Time at 22°C Set-Temperature.

System	HMI	Contact Time (mins)					
		180		270		360	
		q ₁₈₀	%R	q ₂₇₀	%R	q ₃₆₀	%R
[Pb]	Pb ²⁺	0.211	84	0.223	90	0.230	92
[Pb-Cu]	Pb ²⁺	0.116	93	0.119	95	0.120	97
	Cu ²⁺	0.025	20	0.031	25	0.034	27
	TOTAL	0.141	-	0.150	-	0.155	-
[Pb-Fe]	Pb ²⁺	0.109	87	0.114	92	0.118	94
	Fe ³⁺	0.054	43	0.060	48	0.064	52
	TOTAL	0.163	-	0.174	-	0.182	-
[T]	Pb ²⁺	0.076	92	0.079	95	0.080	96
	Cu ²⁺	0.018	21	0.022	27	0.025	30
	Fe ³⁺	0.041	49	0.046	55	0.049	59
	TOTAL	0.135	-	0.147	-	0.153	-
[M]	Pb ²⁺	0.047	95	0.048	97	0.049	97
	Cu ²⁺	0.013	26	0.015	30	0.016	33
	Fe ³⁺	0.029	59	0.031	63	0.033	67
	Ni ²⁺	0.005	9.6	0.005	9.8	0.005	10
	Zn ²⁺	0.011	22	0.013	25	0.014	28
	TOTAL	0.106	-	0.112	-	0.117	-

When the uptake data (in meq/g) of Table 5 is compared to the contact time observations in Table 6 at 180 contact min, the removal efficiency is similarly on trend. Only a 5.94% average percent difference in the uptake of total HMIs of [Pb], [T], and [M] is detected. When this same comparison is made with 20°C uptake of [T] and [M] data of Table 7 (a temperature below the controlled 22°C), only a 4.85% average percent difference in the uptake of total HMIs is detected. These observations demonstrate continuity and repeatability of the experimental procedure.

To visualize the influence of both operating parameters, Figure 3 and Figure 4 display the total HMI uptake (meq/g) with respect to extrapolated contact time and set-temperature, respectively.

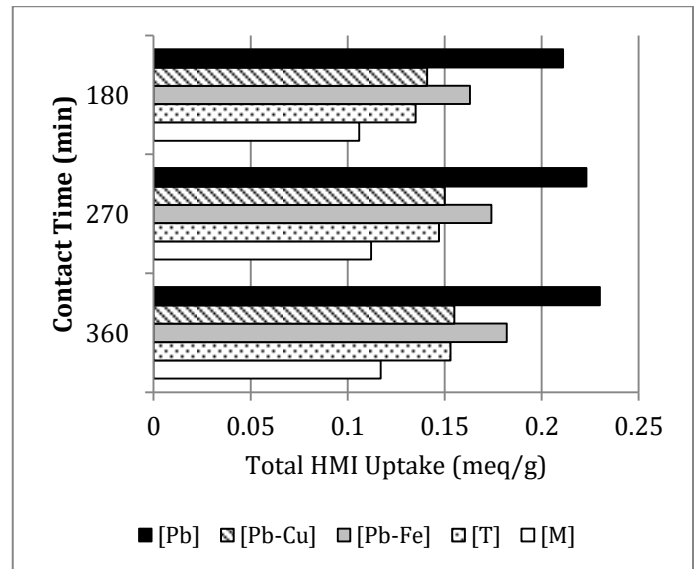


Figure 3. Total HMI Uptake based on Contact Time Parameter.

Table 7. The HMI Removal Variation by Set-Temperature at 180 Contact Min.

System	HMI	Set-Temperature (°C)							
		20		24		28		32	
		q ₁₈₀	%R	q ₁₈₀	%R	q ₁₈₀	%R	q ₁₈₀	%R
[T]	Pb ²⁺	0.075	91	0.076	92	0.076	92	0.077	93
	Cu ²⁺	0.018	22	0.019	23	0.020	24	0.022	27
	Fe ³⁺	0.041	50	0.041	49	0.043	52	0.045	54
	TOTAL	0.135	-	0.137	-	0.140	-	0.144	-
[M]	Pb ²⁺	0.047	95	0.048	95	0.048	95	0.048	96
	Cu ²⁺	0.013	25	0.014	28	0.014	28	0.015	30
	Fe ³⁺	0.030	60	0.030	60	0.031	62	0.031	63
	Ni ²⁺	0.006	13	0.007	13	0.007	13	0.007	13
	Zn ²⁺	0.011	22	0.012	25	0.013	25	0.014	27
	TOTAL	0.107	-	0.111	-	0.112	-	0.114	-

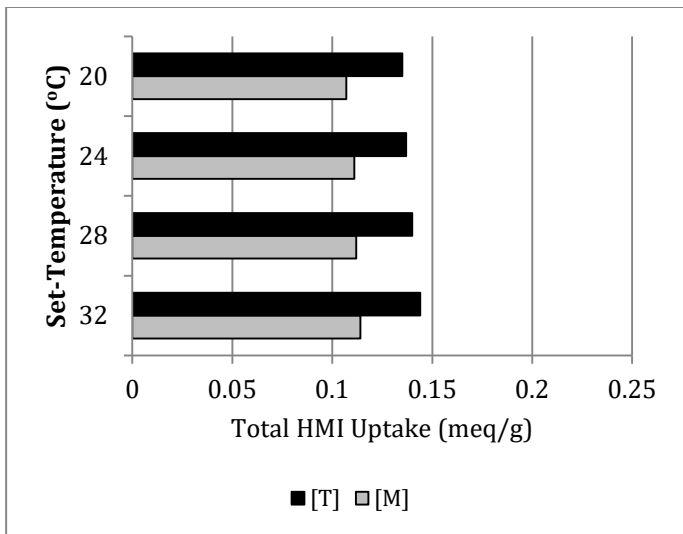


Figure 4. Total HMI Uptake based on Set-Temperature Parameter.

A greater increase in uptake of the total HMIs occurs from 180 to 270 min by, on average 0.010 meq/g compared to 0.006 meq/g from 270 to 360 min. This demonstrates the expected proportionality between uptake and contact time. For Pb^{2+} , the theoretical $q_{e,[Pb]}$ of 0.2440 meq/g by the PSO model (Table 4) is experimentally supported by the q_{360} of 0.230 meq/g. Research conducted by Oter and Akcay [35] demonstrates that equilibrium is attained for Cu^{2+} and Zn^{2+} in approximately 6 contact hr, while more rapidly for Pb^{2+} and Ni^{2+} at only 1 contact hr. As such, the uptake threshold quickly approaches equilibrium at 360 min of contact.

The results in Table 7 are on trend, with the direct proportionality between the systematic increase in set-temperature and uptake. This supports the fact that the sorbent's structure and surface functional groups are influenced by temperature between 20-35°C, observed by the overall sorption capacity [4]. However, the impact of set-temperature is not as significant within this selected range of study conditions.

3. 4. Heat Pre-Treatment

The hydrothermal stability of zeolites establishes the operational lifetime of a material, as well as degradation and regeneration conditions [39]. It is a measure of the structural changes that occur when exposed to water vapour at high temperatures and pressures [40]. This characteristic depends primarily on the type of zeolite, the silica/aluminum ratio, as well as the divalent/monovalent ratio and nature of cations

entering the framework [39,41]. The dehydration process is related to the considerable energy required to break bonds holding water molecules in the intracrystalline channels of zeolite, as well as to overcome the energy barrier with diffusion of water molecules in the channels of the framework. The structural changes that occur are influenced by the degree of participation of water molecules in the energy balance of zeolite. Therefore, water molecules positioned in cavities and channels of the zeolite framework contribute to the compensation of the non-uniformly distributed charge of the silicate framework and cations. When water is separated from the crystalline lattice, the charge distribution breaks down. This leads to a deformation of the framework and variation in the mobile cations' positions [39].

Motsi et al. [1] investigates the uptake efficiency of natural zeolite for the heavy metallic ions (HMIs) Fe^{3+} , Cu^{2+} , Mn^{2+} and Zn^{2+} . The effects of heat pre-treatment are examined with the exposure to a muffle furnace at 200°C, 400°C, and 800°C for 30 mins. The pre-treated zeolite is then in contact with the HMIs in single-component solutions for 6 hrs. It is observed that the specific surface area is improved when treated at 200°C. An increase in both the adsorption rate and capacity due to this thermal treatment is caused by the removal of water from internal channels, which leave them vacant [1]. However, this trend is minimized beyond this temperature threshold. The structure collapses and the porosity inevitably decreases. The rate of adsorption by calcined zeolite is faster compared to untreated zeolite, but the efficiency decreases for zeolite exposed to very high temperatures.

The dehydration of zeolite occurs at a temperature that significantly exceeds the boiling point of water. A considerable amount of water is removed continuously and reversibly, both partially and completely [39,41], when exposed to heat from air at room temperature. When exposed to heat at approximately 350-400°C [12,41,43], the water is eliminated, and the cations fall back into positions on the inner surface of channels and central cavities of the zeolite structure. Dehydration of zeolite is an endothermic process, thereby causing 'activation' of the material [12] between 250-400°C [40] at approximately 350°C [41]; with a structural stability of up to 750°C [41,44]. Research has also revealed that the relationship between the dehydration mechanism of zeolite and positions occupied by aluminum and cations in its structure have an effect on the thermal stability.

Thermal treatment of zeolite between 500-600°C causes the loss of one H₂O for every two tetrahedral aluminum atoms. This temperature range instigates a loss of oxygen atoms in framework, producing structural vacancies [42]. Beyond this thermal threshold, the crystalline structure breaks down and the clinoptilolite becomes an amorphous solid [40,41].

Langelia et al. [42] investigates three thermal behavioural types of zeolites. This work emphasizes that reversible dehydration with minimal framework contraction would be observed upon heating up to approximately 230°C (Type-1) and 280°C (Type-2), while irreversible structural changes hinders rehydration at a range of 230-260°C (Type-1) and 280-400°C (Type-2). Also, heat pre-treatment greater than 450°C (Type-1) and 550°C (Type-2) causes a thermally induced collapse of the zeolite structure. Behavioural Type-3 exhibits continuous reversible dehydration with only very small structural contraction; the framework is not destroyed at an exposure of up to 750°C. High aluminum and alkaline-earth contents give rise to Type-1. An increase in silicon and/or alkaline-earth cations leads to a progressive change in thermal behavior in the order of Type-1 to -2 to -3. The study presented in this paper is also comparable with the findings of Langelia et al. [42], as the temperature levels analyzed exhibit Type-2 behaviour [45].

3. 4. 1. Heavy Metallic Ion Pre-Treatment Trends

Table 8 provides the HMI uptake at 180 min (q_{180} in meq/g) of contact for non-heated and heat-pre-treated zeolite in the triple-[T] and multi-[M] component systems. With each heat pre-treatment level, the same trend is maintained among the various component systems. Once again, for all operation parameters investigated in this study, the zeolite exhibits the highest affinity and favoured uptake for that of the Pb²⁺ ion [4,14,16,21,22,46] followed by Fe²⁺ and Cu²⁺, with a lower affinity to Zn²⁺ then Ni²⁺. A significant loss in crystallinity and hence catalytic activity are common with this pre-treatment process [47]. Dehydration temperature as well as micropore volume and transitional porosity development are directly proportional [40]. It is important to increase surface area, porosity and sorption capacities of natural zeolites without crystallinity loss [47]. The percent removal of the Pb²⁺ ion in [M] is 93.97%, while only 56.70% in [M-600]. The percent removal of the total HMIs reduces from 16.47% to 3.68% going from non-heat-pre-treated to 600°C exposure. This demonstrates

the extreme temperature effects on the zeolite's sorption capacity to the HMIs of interest.

Table 8. HMI Uptake by Heat Pre-Treatment Level.

Heat Level	Non-Heated		200°C		400°C		600°C	
	[T]	[M]	[T]	[M]	[T]	[M]	[T]	[M]
System								
HMI								
Pb ²⁺	0.075	0.047	0.073	0.047	0.057	0.040	0.038	0.028
Cu ²⁺	0.016	0.011	0.015	0.011	0.008	0.006	0.006	0.003
Fe ³⁺	0.041	0.028	0.036	0.025	0.024	0.017	0.026	0.017
Ni ²⁺	-	0.005	-	0.004	-	0.004	-	0.003
Zn ²⁺	-	0.008	-	0.008	-	0.004	-	0.002
TOTAL HMI	0.132	0.099	0.124	0.094	0.088	0.071	0.070	0.052

Figure 5 displays the effects of each heat pre-treatment level, with respect to the percentage of non-heated zeolite uptake. Evidently, the presence of each HMI in solution impacts the uptake of the other; as seen by the interference of the Ni²⁺ and Zn²⁺ ions in the [M] component system uptake of the Cu²⁺, Fe³⁺, and Pb²⁺ ions associated with the [T] system. Comparing [T] to [M], the uptake of the Pb²⁺ ion is reduced by 36.2%, 30.4% and 25.9% at the heat pre-treatment levels of 200°C, 400°C, and 600°C, respectively, and 37.5% without heat pre-treatment. When heat-pre-treated to 600°C, the total HMI uptake is reduced by approximately 47% in both systems.

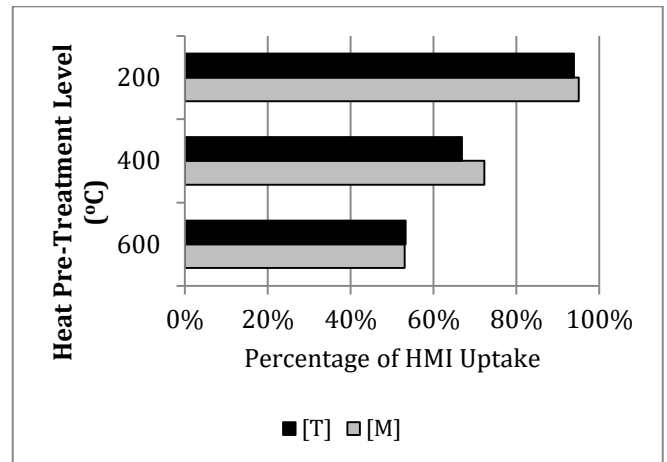
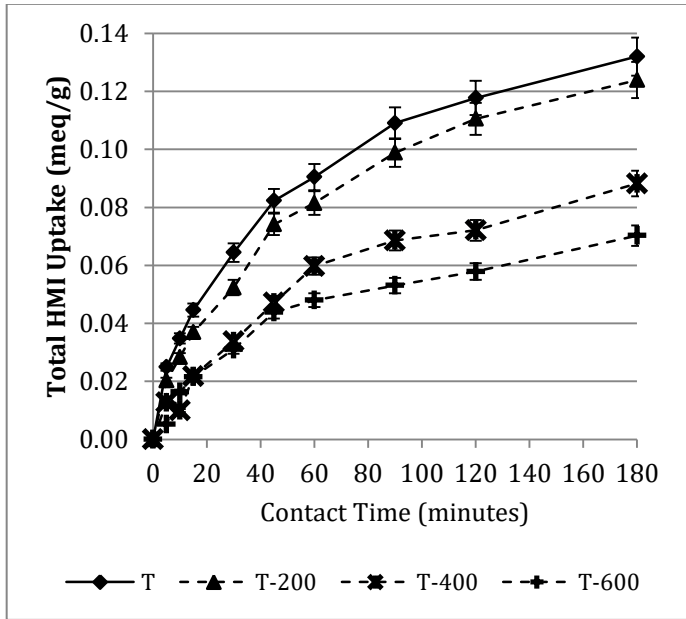


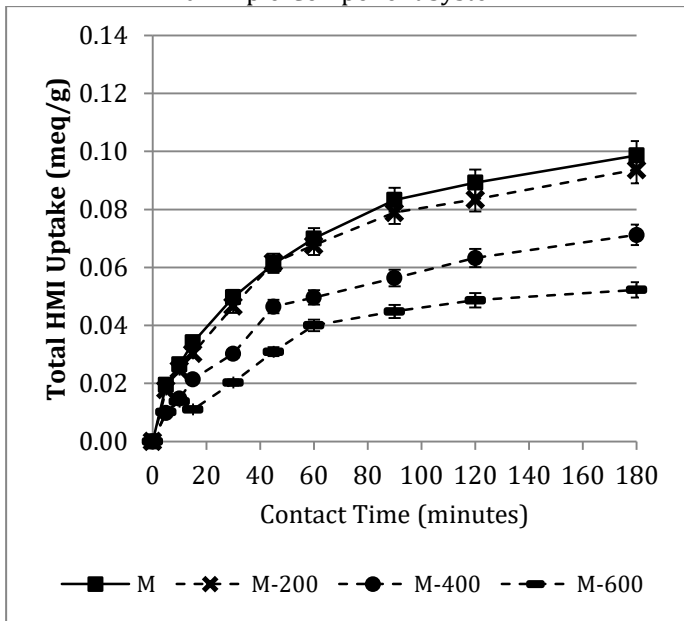
Figure 5. Percentage of Total HMI Uptake Compared to Non-Heated Level.

Figure 6 displays the total HMI uptake over the 3-hr contact period for each heat pre-treatment level, for the [T] (6a.) and [M] (6b.) component systems, respectively. This study is consistent with the three distinct stages discussed by Sprynskyy et al. [4]. As

expected, there is a slightly greater uptake in the [T] over time; attributed to the interference of the additional two HMIs in the [M]. The rate of uptake for both component systems is not significantly affected by the 200°C heat exposure. The first 45-min period is very similar for [M-200], compared to the non-heated. Consistent with the findings of Motsi et al. [1], a substantial reduction of HMI uptake occurs at the 400°C threshold.



a. Triple-Component System



b. Multi-Component System

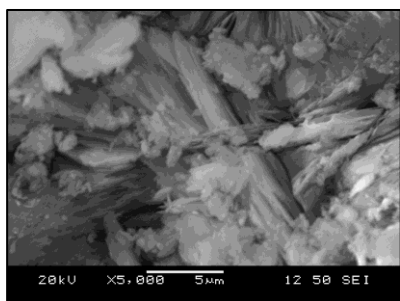
Figure 6. Heat Pre-Treatment Variation of Total HMI Uptake over Time (adapted from [45]).

3. 4. 2. Qualitative Pre-Treatment Trends

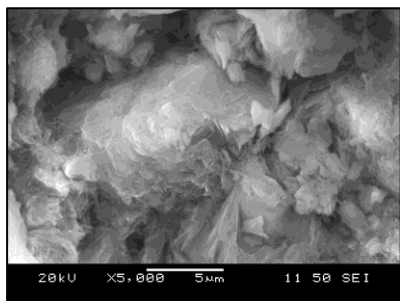
Qualitative analysis of the natural zeolite is conducted to observe the surface topography over time, by a high-resolution Scanning Electron Microscopy (SEM) technology (6380LV, JEOL, USA), equipped with Oxford energy dispersive X-ray spectroscopy (EDS) and electron backscatter diffraction (EBSD) capacity.

Once the cleaning cycle of the raw zeolite sample is complete, the as-received pale green colour is sustained. Following the progressive heat pre-treatment exposure, this colour transitions to a pink, pale pink, then light brown colour [45]. Figure 7 provides SEM images obtained by the high-resolution microscope, taken at $\times 5000$ magnification (5 μm scale bar). Subtle physical changes of the surface structure are observed when comparing the raw granules (shown in 7a.) to those exhibited to the cleaning cycle (shown in 7b.). The images of the zeolite exposed to heat pre-treatment of 200°C, 400°C, and 600°C are shown in 7c., 7d., and 7e., respectively. To point out once again, a substantial reduction of HMI uptake occurs within the 400-600°C temperature range of this study [1]. The non-heated uptake in [T] and [M] is achieved by 93.9% and 95.0% in [T-200] and [M-200], respectively. This is qualitatively observed in Figure 7b. and 7c., with the visual similarity.

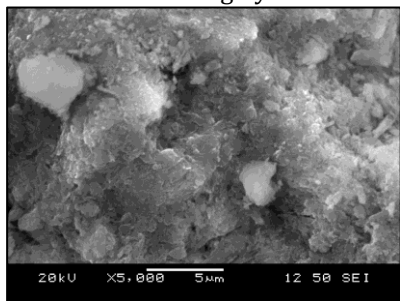
As seen in Table 8, the sorption capacity is significantly compromised at the 400°C and 600°C exposures; which is supported by the lack of textural complexity in Figure 7d. and 7e., respectively. It is visually evident that the raw sample possesses textured granularity and significant detail, which is subsequently diminished with heat-pre-treatment towards the intergranular spaces and mineral crevasses. This provides additional knowledge into how the structure of the zeolite mineral has been modified [45]. However, the process of dehydration requires a considerable amount of energy, which practically outweighs the interest to 'activate' the structure of the mineral sample. Both the quantitative and qualitative observations demonstrate that there is no economic benefit to the hydrothermal pre-treatment of the zeolite mineral, under the testing conditions.



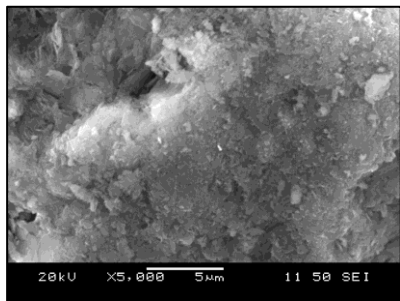
a. Natural Zeolite – As Received



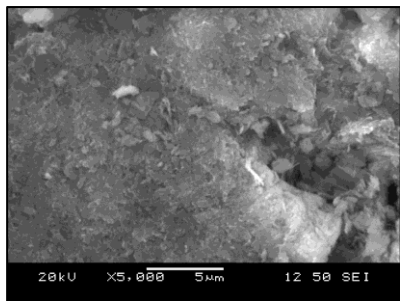
b. Cleaning Cycle



c. Heat Pre-treated at 200°C



d. Heat Pre-treated at 400°C



e. Heat Pre-treated at 600°C

Figure 7. SEM Images of Natural Zeolite Exposure to Heat-Pre-treatment (adapted from [45]).

Innovative treatment technologies are a challenge for all related industry, which include but are not limited to high associated economic costs and pollutant specific methods. Consequently, the conversion of inorganic ion exchangers into hybrid fibrous or nanoscale ion exchangers is considered to be the latest development of the water treatment industry. These materials are gaining attention, as they demonstrate a high efficiency and rate of sorption with short diffusion path towards environmental pollutants. Among metal-containing nanoparticles, carbonaceous materials and dendrimers, zeolites are considered as one of the most progressive functional and nano-sized materials of the millennium. The prospects of this mineral are promising, and its unique position is attributed to its sorption properties particularly through their surface treatment. Nanoscale science and engineering developments are providing extraordinary opportunities to develop more cost effective and environmentally acceptable water purification processes [48].

3. 5. Acidity Observations

It is important to note that the pH level of every ICP-AES sample (stock solution and sorbent-solution contact) is measured for all operating parameters investigated; utilizing the accumet Basic AB15 pH Meter (Fisher Scientific; CAT No. 13 636 AB15). This is conducted after batch mode contact, and before dilution (following 24 hr storage) in preparation for calibration. The set-up of the initial stock pH level is kept consistent throughout all experiments; an average of 1.85 is detected. The average maximum and minimum values between the batch bottle and stored supernatant samples are summarized in Table 9.

Table 9. The Average pH Level Data.

Observation	pH Sample	
	Batch Contact	Storage Filter
Maximum	2.18	2.14
Minimum	1.90	1.89

This data is based on a Dosage 40 ratio (4 g/100 mL); excluding the pH observations for the Dosage 80 (8 g/100 mL) parameter. At 45 min of contact for all HMIs at Dosage 80 conditions, the effluent becomes more basic to reach a pH level of just above 2.20. Overall, the samples collected show an average pH level maximum and minimum of 2.39 and 1.91, respectively. This level is still quite acidic, and is well within the

typical 2 to 5 range as investigated in the Canada-Wide AMD Survey [17]. This brings attention to the fact that the H⁺ ions are in competition with the HMI of interest [15,16]. The doubled dosage provides greater active sites availability for sorption to occur. The decision to proceed with particle size D (d_{p,D}) as the controlled parameter in the analysis is justified, given that the pH level was kept consistent to the completion of this study.

4. Conclusions

The removal efficiency of heavy metallic ions by natural zeolite increases by:

- Decreasing particle size and influent concentration;
- Increasing dosage level, contact time and set-temperature, and by;
- Maintaining the heat-pre-treatment within limits of the activation threshold.

The efficiency is improved depending on the specific metal and the parameter observed. Since the heavy metals selected in this present study possess different chemical and physical properties influenced in the same manner, it can be qualitatively speculated that other heavy metals would be equally influenced [46]. The removal efficiency order (or selectivity series) is consistent for all examined experimental conditions: Pb²⁺>>Fe³⁺>Cu²⁺>Zn²⁺>Ni²⁺ [22,45].

The sorption uptake of HMIs by natural zeolite is complex, due to the aqueous chemistry of the elements and the nature of the sorbent mineral [35]. However, this research provides a greater insight into how the presence of multiple metallic ions and various operative parameters impact the overall removal efficiency, and indicates how the sorption properties of zeolite influence the overall selectivity trends. This is a significant contribution to the current knowledge-base, and how these parameters impact the natural mineral batch mode, for the scale-up to continuous column design and configuration for industrial treatment applications.

References

- [1] T. Motsi, N. A. Rowson, M. J. H. Simmons, "Adsorption of heavy metals from acid mine drainage by natural zeolite," *International Journal of Mineral Processing*, vol. 92, no. 1-2, pp. 42-48, 2009. DOI: 10.1016/j.minpro.2009.02.005.
- [2] A. Akcil, S. Koldas, "Acid Mine Drainage (AMD): Causes, treatment and case studies," *Journal of Cleaner Production*, vol. 14, pp. 1139-1145, 2006. DOI: 10.1016/j.jclepro.2004.09.006.
- [3] E. Erdem, N. Karapinar, R. Donat, "The removal of heavy metal cations by natural zeolites," *Journal of Colloid and Interface Science*, vol. 280, pp. 309-314, 2004. DOI: 10.1016/j.jcis.2004.08.028.
- [4] M. Sprynskyy, B. Buszewski, A. P. Terzyk, J. Namiesnik, "Study of the selection mechanism of heavy metal (Pb²⁺, Cu²⁺, Ni²⁺, and Cd²⁺) adsorption on clinoptilolite," *Journal of Colloid Interface Science*, vol. 304, pp. 21-28, 2006. DOI: 10.1016/j.jcis.2006.07.068.
- [5] M. A. Acheampong, R. J. W. Meulepas, P. N. L. Lens, "Removal of heavy metals and cyanide from gold mine wastewater," *Journal of Chemical Technology and Biotechnology*, vol. 85, pp. 590-613, 2010. DOI: 10.1002/jctb.2358.
- [6] C. Wang, J. Li, X. Sun, L. Wang, X. Sun, "Evaluation of zeolites synthesized from fly ash as potential adsorbents for wastewater containing heavy metals," *Journal of Environmental Sciences*, vol. 21, pp. 127-136, 2009. DOI: 10.1016/S1001-074260022-X.
- [7] T. Motsi, N. A. Rowson, M. J. H. Simmons, "Kinetic studies of the removal of heavy metals from acid mine drainage by natural zeolite," *International Journal of Mineral Processing*, vol. 101, pp. 42-49, 2011. DOI: 10.1016/j.minpro.2011.07.004.
- [8] L. Curkovic, S. Cerjan-Stefanovic, T. Filipan, "Metal ion exchange by natural and modified zeolites," *Water Research*, vol. 31, no. 6, pp. 1379-1382, 1997. DOI: 10.1016/S0043-135400411-3.
- [9] F. Helfferich, *Ion Exchange. Series in Advanced Chemistry*. McGraw-Hill, New York, USA, 1962, pp. 95-322.
- [10] V. J. Inglezakis, S. G. Pouloupoulos, "Adsorption and Ion-Exchange (Kinetics)," *In Adsorption, Ion Exchange and Catalysis, Design of Operations and Environmental Applications*, 1st ed., Elsevier Science: Amsterdam, The Netherlands, 2006, pp. 262-266. ISBN-13: 978-0-444-52783-7.
- [11] G. V. Tsitsishvili, "Perspectives of Natural Zeolite Applications," *Occurrences, Properties and Utilization of Natural Zeolites*, Akademiai Kiado: Budapest, Hungary, 1988, pp. 367-393.
- [12] F. A. Mumpton, J. R. Boles, E. M. Flanigen, A. J. Gude, R. A. Sheppard, R. L. Hay, R. C. Surdam, *Mineralogy and Geology of Natural Zeolites*. Washington, D.C.: Mineralogical Society of America, 1977, pp. 165. ISBN: 0939950049.

- [13] S. Wang, Y. Peng, "Natural zeolites as effective adsorbents in water and wastewater treatment," *Chemical Engineering Journal*, vol. 156, pp. 11-24, 2010. DOI: 10.1016/j.cej.2009.10.029.
- [14] V. J. Inglezakis, M. D. Loizidou, H. P. Grigoropoulou, "Equilibrium and kinetic ion exchange studies of Pb^{2+} , Cr^{3+} , Fe^{3+} and Cu^{2+} on natural clinoptilolite," *Water Research*, vol. 36, pp. 2784-2792, 2002. DOI: 10.1016/S0043-135400504-8.
- [15] B. Ersoy, M. S. Celik, "Electrokinetic properties of clinoptilolite with mono- and multivalent electrolytes," *Microporous and Mesoporous Materials*, vol. 55, pp. 305-312, 2002. DOI: 10.1016/S1387-181100433-X.
- [16] V. J. Inglezakis, M. D. Loizidou, H. P. Grigoropoulou, "Ion exchange of Pb^{2+} , Cu^{2+} , Fe^{3+} , and Cr^{3+} on natural clinoptilolite: selectivity determination and influence of acidity on metal uptake," *Journal of Colloid Interface Science*, vol. 261, pp. 49-54, 2003. DOI: 10.1016/S0021-979700244-8.
- [17] L. J. Wilson. (2014, October 30). "Canada-Wide Survey of Acid Mine Drainage Characteristics. Project Report 3.22.1-Job No. 50788," Mineral Sciences Laboratories Division Report MSL 94-32 (CR), Ontario Ministry of Northern Development and Mines. Mine Environment Neutral Drainage (MEND) Program, Canada, 1994. [Online]. Available: <http://mend-nedem.org/wp-content/uploads/2013/01/3.22.1.pdf>
- [18] H. Cui, L. Y. Li, J. R. Grace, "Exploration of remediation of acid rock drainage with clinoptilolite as sorbent in a slurry bubble column for both heavy metal capture and regeneration," *Water Research*, pp. 3359-3366, 2006. DOI: 10.1016/j.watres.2006.07.028.
- [19] T. Motsi, "Remediation of Acid Mine Drainage using Natural Zeolite," Ph.D. Thesis, School of Chemical Engineering, The University of Birmingham, United Kingdom, 2010.
- [20] W. Xu, L. Y. Li, J. R. Grace, G. Hebrard, "Acid rock drainage treatment by clinoptilolite with slurry bubble column: Sustainable zinc removal with regeneration of clinoptilolite," *Applied Clay Science*, vol. 80-81, pp. 31-37, 2013. DOI: 10.1016/j.clay.2013.05.009.
- [21] V. J. Inglezakis, H. Grigoropoulou, "Effects of operating conditions on the removal of heavy metals by zeolite in fixed bed reactors," *Journal of Hazardous Materials*, vol. 112, pp. 37-43, 2004. DOI: 10.1016/j.jhazmat.2004.02.052.
- [22] A. L. Ciosek, G. K. Luk, "Lead Removal from Mine Tailings with Multiple Metallic Ions," *International Journal of Water and Wastewater Treatment*, vol. 3, pp. 1-9, 2017. DOI: 10.16966/2381-5299.134.
- [23] A. L. Ciosek, G. K. Luk, "Kinetic Modelling of the Removal of Multiple Heavy Metallic Ions in Mine Waste by Natural Zeolite Sorption," *Special Issue: Treatment of Wastewater and Drinking Water through Advanced Technologies, In Water*, vol. 9, no. 7, pp. 482, 2017. DOI: 10.3390/w9070482.
- [24] A. L. Ciosek, G. K. Luk, "An Innovative Dual-Column System for Heavy Metallic Ion Sorption by Natural Zeolite," *Special Issue: Wastewater Treatment and Reuse Technologies, In Applied Sciences*, vol. 7, no. 8, pp. 795, 2017. DOI: 10.3390/app7080795.
- [25] Canadian Minister of Justice (CMJ). *Metal Mining Effluent Regulations. Consolidation SOR/2002-222*. 2014. [Online]. Available: <http://laws-lois.justice.gc.ca>
- [26] H. V. Bekkum, E. M. Flanigen, J. C. Jansen, "Ion-Exchange in Zeolites" *In Introduction to Zeolite Science and Practice—Studies in Surface Science and Catalysis*, 1st ed., Elsevier Science: Zeist, The Netherlands, vol. 58, 1991, pp. 359-390.
- [27] E. W. Rice, R. B. Baird, A. D. Eaton, L. S. Clesceri, "Part 1000-Introduction, Part 3000-METALS," *In Standard Methods for the Examination of Water and Wastewater*, 22nd ed., APHA, AWWA, WEF: Washington DC, USA, 2012, pp. 1.1-68; 3.1-112, ISSN: 978-087553-013-0.
- [28] M. Minceva, R. Fajgar, L. Markovska, V. Meshko, "Comparative Study of Zn^{2+} , Cd^{2+} , and Pb^{2+} Removal From Water Solution Using Natural Clinoptilolitic Zeolite and Commercial Granulated Activated Carbon: Equilibrium of Adsorption," *Separation Science and Technology*, vol. 43, pp. 2117-2143, 2008. DOI: 10.1080/01496390801941174.
- [29] U. Wingenfelder, C. Hansen, G. Furrer, R. Schulin, "Removal of Heavy Metals from Mine Waters from Natural Zeolites," *Environmental Science and Technology*, vol. 39, no 12, pp. 4606-4613, 2005. DOI: 10.1021/es048482s.
- [30] Bear River Zeolite Co. Inc. (2012 and 2017, September 1). *Zeolite-Specifications and MSDS*. [Online]. Available: <http://www.bearriverzeolite.com>
- [31] V. J. Inglezakis, C. D. Papadeas, M. D. Loizidou, H. P. Grigoropoulou, "Effects of Pretreatment on

- Physical and Ion Exchange Properties of Natural Clinoptilolite,” *Environmental Technology*, vol. 22, pp. 75-82, 2001. DOI: 10.1080/09593332208618308.
- [32] Perkin Elmer Inc., *Atomic Spectroscopy—A Guide to Selecting the Appropriate Technique and System: World Leader in AA, ICP-OES, and ICP-MS*, Perkin Elmer Inc., Waltham MA, USA, 2011.
- [33] Perkin Elmer Inc., *WinLab32 for ICP—Instrument Control Software, version 5.0*, Perkin Elmer Inc., Waltham MA, USA, 2010.
- [34] J. Mullin, “Physical and thermal properties,” In *Crystallization*, 4th ed., Read Educational and Professional Publishing Ltd., Woburn, MA, USA, pp. 76-77, 2001. ISBN: 0-7506-4833-3.
- [35] O. Oter, H. Akcay, “Use of Natural Clinoptilolite to Improve Water Quality: Sorption and Selectivity Studies of Lead(II), Copper(II), Zinc(II), and Nickel(II),” *Water Environment Research*, vol. 79, no. 3, pp. 329-335, 2007. DOI: 10.2175/106143006X111880.
- [36] H. Qiu, L. Lv, B. C. Pan, Q. J. Zhang, W. M. Zhang, Q. X. Zhang, “Critical review in adsorption kinetic models,” *Journal of Zhejiang University Science A*, vol. 10, pp. 716-724, 2009. DOI: 10.1631/jzus.A0820524.
- [37] N. Bektas, S. Kara, “Removal of lead from aqueous solutions by natural clinoptilolite: Equilibrium and kinetic studies,” *Separation and Purification Technology*, vol. 39, pp. 189-200, 2004. DOI: 10.1016/j.seppur.2003.12.001.
- [38] Y. Ho, A. E. Ofomaja, “Pseudo-second-order model for lead ion sorption from aqueous solutions onto palm kernel fiber,” *Journal of Hazardous Materials*, vol. 129, pp. 137-142, 2005. DOI: 10.1016/j.jhazmat.2005.08.020.
- [39] M. Jovanovic, N. Rajic, B. Obradovic, “Novel kinetic model of the removal of divalent heavy metal ions from aqueous solutions by natural clinoptilolite,” *Journal of Hazardous Materials*, vol. 233, pp. 57-64, 2012. DOI: 10.1016/j.jhazmat.2012.06.052.
- [40] M. N. Kostandyan, S. G. Babayan, M. A. Balayan, “Effect of heat treatment on the structural characteristics and sorption properties of clinoptilolite,” *Inorganic Materials*, vol. 18, no. 10, 0020-1685, pp. 1498 -1501, 1982.
- [41] D. W. Breck, *Zeolite Molecular Sieves: Structure, Chemistry, and Use*. John Wiley & Sons, New York, 1974.
- [42] A. Langelia, M. Pansini, G. Cerri, P. Cappellietti, M. De Gennaro, “Thermal Behavior of Natural and Cation-Exchanged Clinoptilolite from Sardinia (Italy),” *Clays and Clay Minerals*, vol. 51, no. 6, pp. 625-633, 2003. DOI: 10.1346/CCMN.2003.0510605.
- [43] E. Yörükoğulları, G. Yılmaz, S. Dikmen, “Thermal treatment of zeolitic tuff,” *Journal of Thermal Analysis and Calorimetry*, vol. 100, no. 3, pp. 925-928, 2010. DOI: 10.1007/s10973-009-0503-8.
- [44] K. Margeta, N. Zabukovec Logar, M. Šiljeg; A. Farkaš, “Natural Zeolites in Water Treatment—How Effective Is Their Use,” *InTech, Water Treatment W. Elshorbagy*, Ed., pp. 81-112, 2013. DOI: 10.5772/50738.
- [45] A. L. Ciosek, G. K. Luk, “Effects of Heat Pre-Treatment on Metallic Ion Sorption by Natural Zeolite,” *Technical Session: Industrial Treatment A, Water Environment Association of Ontario Technical Symposium and OPCEA Exhibition*, Ottawa, Canada, 2017. Paper No: 2017-010.
- [46] S. K. Ouki, M. Kavannagh, “Performance of natural zeolites for the treatment of mixed metal contaminated effluents,” *Waste Management and Research*, vol. 15, no. 4, pp. 383-394, 1997. DOI: 10.1006/wmre.1996.0094.
- [47] D. B. Akkoca, M. Yilgin, M. Ural, H. Akcin, A. Mergen, “Hydrothermal and Thermal Treatment of Natural Clinoptilolite Zeolite from Bigadiç, Turkey: An Experimental Study,” *Geochemistry International*, vol. 51, no. 6, pp. 495-504, 2013. DOI: 10.1134/S0016702913040022.
- [48] E. Chmielewska, L. Sabová, K. Jesenák, “Study of adsorption phenomena ongoing onto clinoptilolite with the immobilized interfaces,” *Journal of Thermal Analysis and Calorimetry*, vol. 92, no. 2, pp. 567-571, 2008. DOI: 10.1007/s10973-006-8315-6.